Acta Biochim Biophys Sin 2023, 55(9): 1370–1379
https://doi.org/10.3724/abbs.2023155
Advance Access Publication Date: 15 August 2023
Original Article

Original Article

PGAM5 deacetylation mediated by SIRT2 facilitates lipid metabolism and liver cancer proliferation

Gongyu Fu[1,2,†], Shi-Ting Li[3,†], Zetan Jiang[1,2,†], Qiankun Mao[1,2], Nanchi Xiong[1,2], Xiang Li[2], Yijie Hao[1,2,*], and Huafeng Zhang[1,2,*]

[1]Anhui Key Laboratory of Hepatopancreatobiliary Surgery, Department of General Surgery, Anhui Provincial Hospital, the First Affiliated Hospital of USTC, Division of Life Science and Medicine, University of Science and Technology of China, Hefei 230027, China, [2]Hefei National Laboratory for Physical Sciences at Microscale, the Chinese Academy of Sciences Key Laboratory of Innate Immunity and Chronic Disease, School of Basic Medical Sciences, Division of Life Science and Medicine, University of Science and Technology of China, Hefei 230027, China, and [3]Guangdong Cardiovascular Institute, Guangdong Provincial People's Hospital, Guangdong Academy of Medical Sciences, Guangzhou 510080, China

[†]These authors contributed equally to this work.

*Correspondence address. Tel: +86-18298002506; E-mail: biohyj@mail.ustc.edu.cn (Y.H.) / Tel: +86-551-63607012; E-mail: hzhang22@ustc.edu.cn (H.Z.)

Received 25 September 2022 Accepted 13 February 2023

Abstract

Tumor metabolic reprogramming and epigenetic modification work together to promote tumorigenesis and development. Protein lysine acetylation, which affects a variety of biological functions of proteins, plays an important role under physiological and pathological conditions. Here, through immunoprecipitation and mass spectrum data, we show that phosphoglycerate mutase 5 (PGAM5) deacetylation enhances malic enzyme 1 (ME1) metabolic enzyme activity to promote lipid synthesis and proliferation of liver cancer cells. Mechanistically, we demonstrate that the deacetylase SIRT2 mediates PGAM5 deacetylation to activate ME1 activity, leading to ME1 dephosphorylation, subsequent lipid accumulation and the proliferation of liver cancer cells. Taken together, our study establishes an important role for the SIRT2-PGAM5-ME1 axis in the proliferation of liver cancer cells, suggesting a potential innovative cancer therapy.

Key words metabolic reprograming, PGAM5, protein acetylation, SIRT2, ME1, liver cancer

Introduction

Lysine acetylation was originally identified as a major post-translational modification of histones and plays a key role in the regulation of gene expression. Recent studies have also identified acetylated non-histone proteins and extranuclear acetylation-modifying enzymes for regulating a wide range of cellular processes [1,2]. Moreover, a great number of acetylation-modifying enzymes that catalyze intermediate metabolism have been discovered to directly affect enzyme activity and/or stability, which is critical for metabolic regulation in response to alterations in extracellular nutrient availability [3,4]. Increasing evidence has demonstrated that the reversible acetylation of metabolic enzymes is involved in modulating cancer cell metabolism, an emerging hallmark of tumorigenesis [5,6]. However, little is known about the enzymes involved in modulating lysine acetylation-mediated metabolic reprogramming and tumor progression.

Phosphoglycerate mutase 5 (PGAM5) belongs to the phosphoglycerate mutase family. In contrast to other family members, PGAM5 functions as a serine/threonine protein phosphatase rather than a phosphoglycerate mutase [7]. PGAM5 is involved in apoptotic and necroptotic pathways through mitophagy induced by mitochondrial damage [8–11]. PGAM5 is also upregulated in many cancers and promotes their growth [12,13]. Interestingly, Zhu *et al*. [14] recently reported that PGAM5 is highly expressed in colorectal cancer, and the inhibition of PGAM5 expression attenuates lipid metabolism and colon tumorigenesis in mice. The dephosphorylation of malic enzyme 1 (ME1) at S336 mediated by PGAM5 results in the dimerization and activation of ME1 and promotes nicotinamide adenine dinucleotide phosphate (NADPH) production, adipogenesis, and colorectal cancer progression [14]. Although PGAM5 is highly expressed in many cancers, the acetylation of PGAM5 and its regulatory mechanism

have not been reported in liver cancer cells. How it participates in the metabolic reprogramming of liver cancer deserves further study.

We and others have previously discovered that lysine acetylation is an evolutionarily conserved post-translational modification in the regulation of a variety of cellular processes, particularly in mitochondrial metabolism [3,15]. Among these newly identified acetylated proteins, PGAM5 was implicated in new regulation at the post-translational level. In this study, we investigated PGAM5 acetylation and its functional significance in controlling NADPH production and adipogenesis in liver cancer cells.

Materials and Methods

Cell culture and reagents

HEK293T cells (human embryonic kidney cells) and PLC cells (human hepatocarcinoma cell line) were purchased from ATCC (Manassas, USA). All cell lines were cultured in DMEM (Gibco, Carlsbad, USA) supplemented with 10% fetal bovine serum (FBS; Viva-Cell, Shanghai, China) and 1% penicillin-streptomycin (HyClone, Logan, USA) and were tested for mycoplasma contamination to ensure the reliability of the experimental data. All cell lines were incubated at 37°C with 5% CO_2. Nicotinamide (NAM; N0636) and trichostatin A (TSA; V900931) were purchased from Sigma-Aldrich (St Louis, USA).

Plasmids

shRNAs in the PLKO.1 vector against human SIRT2 were commercially purchased from Sigma-Aldrich. shRNAs targeting the 3′UTR of PGAM5 were constructed in the PLKO.1 vector. All shRNA targeting sequences are listed in Supplementary Table S1. The coding sequences of human PGAM5, PGAM5^{K30R}, PGAM5^{K88R}, PGAM5$^{K75R/K88R/K93R/K95R/K116R}$, PGAM5^{K141R}, PGAM5^{K144R}, PGAM5^{K169R}, PGAM5^{K191R}, PGAM5^{K285R}, ME1, and ME1^{S336A} were cloned into the pCDH empty vector (#192245; Addgene, Watertown, USA) with a 3× Flag tag at the C-terminus. The coding sequences of SIRT2, PGAM5, PGAM5^{K191R}, PGAM5^{K191Q}, and ME1 were cloned into the pSIN empty vector (#16580; Addgene) with an HA tag at the N-terminus.

Lentivirus packaging and establishment of stable cells

To generate lentiviruses expressing the indicated shRNAs, HEK293T cells were transfected with shRNAs (cloned in PLKO.1), VSVG and Δ8.9 using PEI transfection reagent (23966-1; Polysciences, Warrington, USA). To generate lentiviruses expressing the pSin empty vector (control) or the indicated genes, HEK293T cells were transfected with the pSin-based construct pMD2.G, and psPAX2 using PEI transfection reagent (Polysciences). To generate lentiviruses expressing the pCDH empty vector (control) or the indicated genes, HEK293T cells were transfected with the pCDH-based construct pMD2.G, and psPAX2 using PEI transfection reagent (Polysciences). Six hours after transfection, the culture medium was replaced by fresh medium. Forty-eight hours later, the medium containing lentiviral particles was collected by filtration with a 0.45-μm PVDF membrane (Millipore, Billerica, USA). Briefly, PLC cells were infected with lentivirus in the presence of polybrene, followed by selection with 0.4 μg/mL puromycin to establish stable cells. Stable cell lines were examined for the expression of the indicated vectors by western blot analysis.

Western blot analysis

Proteins were isolated from cells using RIPA buffer (50 mM Tris-HCl, pH 8.0, 150 mM NaCl, 5 mM EDTA, 0.1% SDS, and 1% NP-40) supplemented with protease inhibitor cocktail (#43203100; Roche, Mannheim, Germany) and 1 mM PMSF, 1 mM Na_3VO_4, 2 mM DTT, and 10 mM NaF. The lysate supernatant was collected after centrifugation at 16,000 *g* for 10 min at 4°C, and the protein concentration was quantified with a Bradford assay kit (C000164-0200; Sangon Biotech, Shanghai, China). Then, the sample was placed in a 100°C metal bath for 5 min. Equal amounts of protein were subjected to 6%–12% SDS-PAGE and then transferred to NC membranes (Cat# 66485; Pall, Logan, USA) for antibody incubation and color development. After being blocked with 5% skimmed milk for 1 h, membranes were incubated with primary antibodies overnight at 4°C. Primary antibodies against the following proteins were used: PGAM5 (Cat# sc-515880; Santa Cruz, Santa Cruz, USA), PGAM5 (Cat# 28445-1-AP; Proteintech, Rosemont, USA), SIRT2 (Cat# 19655-1-AP; Proteintech), SIRT2 (Cat# sc-28298; Santa Cruz), ME1 (Cat# 16619-1-AP; Proteintech), acetylated-lysine (Cat# 9441; CST, Beverly, USA), acetylated-lysine (Cat# PTM-105; Jingjie PTM BioLab, Hangzhou, China), phosphorylation-serine (Cat# sc-81514; Santa Cruz), HA-HRP (Cat# 2999; CST), HA (Cat# 51064-2-AP; Proteintech), mouse IgG1 isotype control (Cat# 66360-1-Ig; Proteintech), Flag (Cat# F1804; Sigma-Aldrich), and β-actin (Cat# 66009-1-Ig; Proteintech). After extensive wash for three times, the membranes were incubated with the HRP-conjugated anti-rabbit secondary antibody (Cat# 1706515; Bio-Rad, Hercules, USA) or HRP-conjugated anti-mouse secondary antibody (Cat# 1706516; Bio-Rad) for 2 h at room temperature. Signals were detected using Western ECL Substrate (Bio-Rad) and ChemiDoc XRS$^+$ System (Bio-Rad).

Immunoprecipitation assay

Cells were lysed in IP buffer (20 mM HEPES, pH 7.5, 150 mM NaCl, 2 mM EDTA, 1% NP40) supplemented with protease inhibitors. Fifty to 100 μg of lysate was saved as an input sample for quantitation of total samples. Equivalent amounts of protein were immunoprecipitated with anti-Flag antibody for 4–6 h at 4°C, followed by incubation with protein A/G-Sepharose (Thermo Scientific, Waltham, USA) for 1 h. The beads were washed three times with IP buffer and boiled in 2× loading buffer. Protein samples were analyzed by western blot analysis.

Fusion protein purification experiment

The coding sequences of human PGAM5, PGAM5^{K141R}, PGAM5^{K141Q}, PGAM5^{K191R}, and PGAM5^{K191Q} were cloned into the pET-22b vector (#103000; Addgene). The proteins PGAM5, PGAM5^{K141R}, PGAM5^{K141Q}, PGAM5^{K191R}, and PGAM5^{K191Q} were produced in *E. coli* (Rossetta, DE3). All proteins were purified using purification buffer (150 mM NaCl, 50 mM Tris, pH 7.5, and 200 mM imidazole). Protein samples were analyzed by Coomassie blue staining.

In vitro phosphatase assay

Phosphatase activity was measured using the Serine/Threonine Phosphatase Assay System (Promega, Madison, USA), which determined the absorbance of the molybdate: malachite: phosphate complex. The following phosphor-peptide was used as a substrate: RRA(pT)VA (Promega).

Measurement of malic enzyme 1 enzyme activity

Malic enzyme 1 (ME1) activity was measured using an NADP-ME activity detection kit (BC1125; Solarbio, Beijing, China) according to the manufacturer's instructions. The optimum reaction system was prepared as follows: 50 mM Tris-HCl, pH 7.5, 1 mM $MgCl_2$, 0.5 mM $NADP^+$, and 10 mM L-malate. The soluble protein concentration was quantified using a Bradford Protein Assay Kit (C503031; Sangon Biotech). ME1 activity was determined by monitoring the change in absorbance at 1 min intervals continuously at 340 nm using a UV spectrophotometer (Thermo Scientific). One unit of ME1 activity was defined as 1 μM NADPH generated by 1 mg protein per minute in the reaction system:

$$\text{NADP-ME1(U/mg protein)} = [(A2–A1)/6.22] \times (l/t) \times (V1/V2)/C,$$

where A1 is the initial absorbance, A2 is the absorbance after the reaction, 6.22 represents the extinction coefficient per mM NADPH, t is the reaction time (1 min), l is the path length of the cuvette (1 cm), V1 is the total reaction volume (900 μL), V2 is the volume of ME1 solution (30 μL), and C is the concentration of protein (mg/mL).

NADPH measurement

For NADPH measurement, cells were collected and lysed with RIPA buffer supplemented with 1% NP-40 for 30 min, and an equal volume of cell lysates was used to measure NADPH using an $NADP^+$/NADPH Detection Kit (S0179; Beyotime Biotechnology, Shanghai, China). The NADPH contents were normalized to cellular protein measured with a Bradford Protein Assay Kit (C503031; Sangon Biotech).

Triglyceride measurement

For triglyceride measurement, cells were collected and lysed with RIPA buffer supplied with 1% NP-40 for 30 min, and equal volumes of cell lysates were used to measure triglycerides using a Biochemical Triglyceride Determination Kit (F001-1-1; Nanjing Jiancheng Bioengineering Institute, Nanjing, China). The triglyceride contents were normalized to cellular protein measured with a Bradford protein assay kit (C503031; Sangon Biotech).

Animal studies

Xenograft experiments were conducted with approval from the Animal Research Ethics Committee of the University of Science and Technology of China (USTCACUC24120122074). Male BALB/c nude mice (Zhejiang Vital River Laboratory Animal Technology Co., Ltd, Hangzhou, China) were kept at room temperature under a constant 12 h light/dark cycle. Mice were held five per cage and randomly assigned to experimental groups. For the xenograft experiment, 10×10^6 PLC cells stably expressing PGAM5-WT, PGAM5-K191R or PGAM5-K191Q with endogenous PGAM5 knockdown were injected subcutaneously into 5-week-old male nude mice. Tumors were measured using digital callipers every 3 days after 7 days of injection. Tumor volumes (mm^3) were calculated using the following formula: length × $width^2$ × 0.52.

Crosslinking assay

Disuccinimidyl suberate (DSS) crosslinking was used to detect the ME1 dimer. Briefly, cells were trypsinized and counted. Equal numbers of cells were collected for the experiment. Cells were washed with cold PBS, followed by suspension in conjugation buffer (20 mM HEPES, pH 8.0). The DSS solution prepared in DMSO was added to the cell suspension to a final concentration of 1 mM. After incubation at 37°C for 30 min, the samples were boiled and subjected to western blot analysis.

Statistical analysis

Data are presented as the mean ± SD or mean ± SEM of at least three independent experiments as indicated. Student's *t* test was used to compare two groups. ANOVA was used for multiple comparisons with GraphPad Prism (Graphpad Software, La Jolla, USA). $P < 0.05$ was considered significant.

Results

K191 acetylation reduces PGAM5 activity

As reported, PGAM5, a transmembrane protein, is highly expressed in liver cancer and colorectal cancer, and high expression of PGAM5 can promote the proliferation of tumor cells [12,14,16]. Our recent studies have revealed a broad role of lysine acetylation in metabolic enzyme regulation in mitochondria, including PGAM5 [15]. To confirm this, we transfected Flag-PGAM5 into HEK293T cells and tested the acetylation of PGAM5 by western blot analysis using an anti-pan-lysine acetylation antibody. We found that PGAM5 was indeed acetylated and that its acetylation was significantly enhanced by treatment with TSA and NAM (Figure 1A). Similar results were observed in PGAM5-overexpressing PLC cells treated with TSA and NAM (Figure 1B). These results suggest that ectopically expressed PGAM5 is acetylated in cells.

Analysis of our previous mass spectrum data revealed that K88 and K191 of PGAM5 are the potential acetylation sites [15]. Meanwhile, the online PhosphoSitePlus database (www.phosphosite.org) predicted other putative acetylation sites in PGAM5. To identify the lysine residues on PGAM5 responsible for its acetylation and activity, we mutated all the putative acetylation sites individually to non-acetylated arginine (R) and detected their acetylation levels. However, K141R or K191R mutants resulted in a significant reduction in PGAM5 acetylation (Figure 1C). We next detected the wild-type PGAM5, K141R and K191R mutants in PLC cells and then treated the cells with TSA and NAM. Western blot analysis with an anti-panlysine acetylated antibody showed that the K191R mutation, but not the K141R mutant, decreased the acetylation level of PGAM5 (Figure 1D). To determine whether the acetylation of K141 or K191 affects the protein phosphatase activity of PGAM5, we purified wild-type PGAM5 as well as K141R, K141Q, K191R and K191Q. Our data showed that the K141R and K141Q mutants did not affect PGAM5 activity. However, compared with wild-type PGAM5, the K191Q (acetyl-mimetic) mutant obviously obstructed PGAM5 activity, and the K191R mutant partly increased the activity of PGAM5 (Figure 1E). It should also be noted that K191 on PGAM5 is evolutionarily conserved from *E. coli* to mammals (Figure 1F). Together, these results support the conclusion that the acetylation of K191 on PGAM5 negatively regulates its enzyme activity. Therefore, we investigated the regulatory mechanisms of PGAM5 acetylation.

SIRT2 mediates PGAM5-K191 deacetylation

To identify the deacetylase responsible for PGAM5 regulation, we first took advantage of TSA, an inhibitor of histone deacetylase, and NAM, an inhibitor of the SIRT deacetylase family, to determine whether SIRTs or HDACs are involved in PGAM5 deacetylation. Treatment with the Sirtuin inhibitor NAM, but not the HDAC

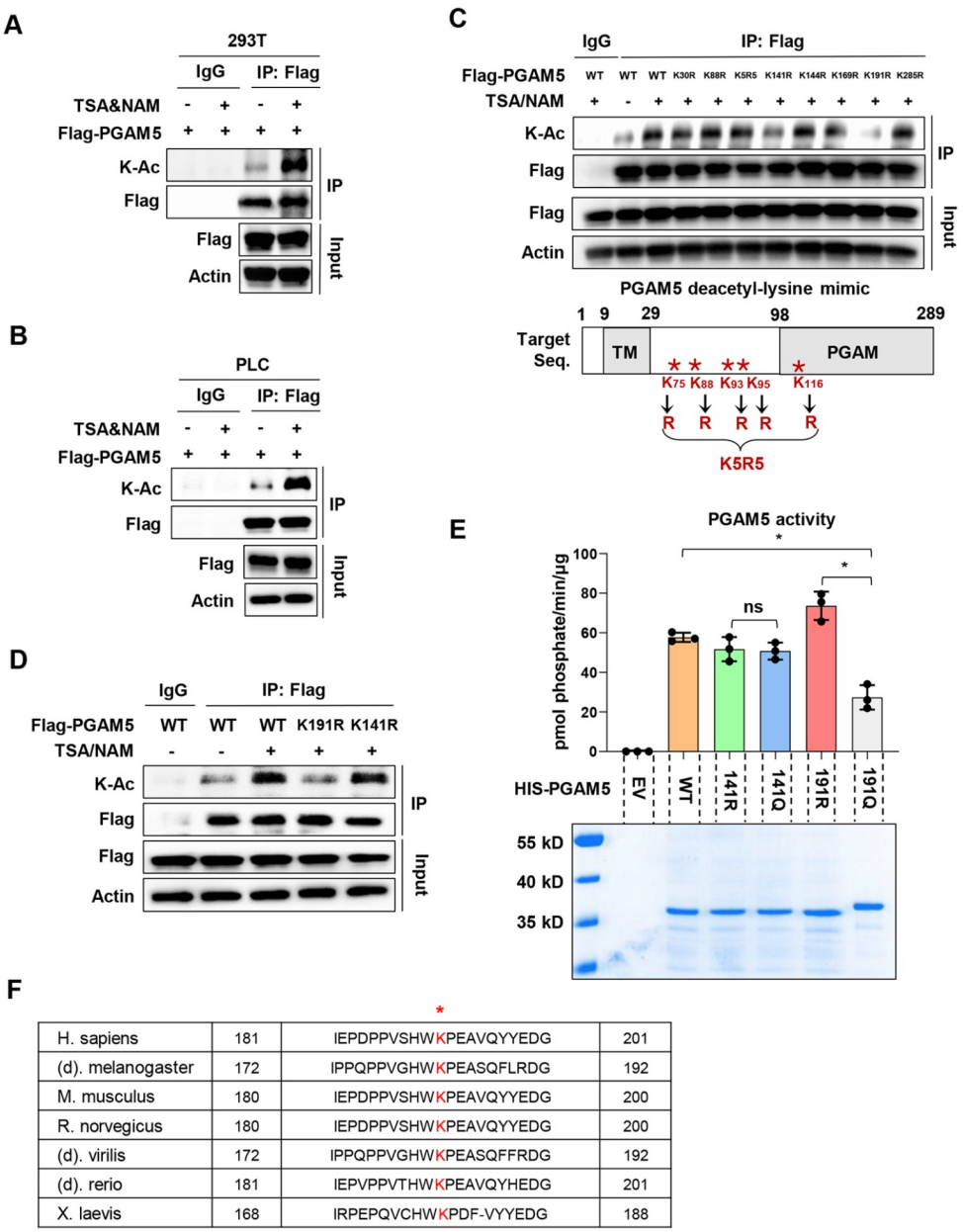

Figure 1. Acetylation at K191 reduces PGAM5 activity (A) Flag-tagged PGAM5 was expressed in HEK293T cells treated with or without the deacetylase inhibitors TSA and NAM, followed by immunoprecipitation using an anti-Flag antibody and western blot analysis of lysine acetylation (K-Ac) of PGAM5. (B) Flag-tagged PGAM5 was stably expressed in PLC cells treated with or without the deacetylase inhibitors TSA and NAM, followed by immunoprecipitation using an anti-Flag antibody and western blot analysis of lysine acetylation (K-Ac) of PGAM5. (C) The indicated mutant plasmids of the PGAM5 acetylation sites were constructed and transfected into HEK293T cells. The above cells were treated with the deacetylase inhibitors TSA and NAM, followed by immunoprecipitation using an anti-Flag antibody and western blot analysis of the PGAM5 acetylation level. (D) PLC cells were transfected with vectors expressing Flag-wild-type-PGAM5 (WT), Flag-PGAM5-K141R (K141R) or Flag-PGAM5-K191R (K191R). The above cells were further treated with the deacetylase inhibitors TSA and NAM, followed by immunoprecipitation using an anti-Flag antibody and western blot analysis of the PGAM5 acetylation level. (E) Bacterially generated HIS-wild-type-PGAM5 (WT), HIS-PGAM5-K141R (K141R), HIS-PGAM5-K141Q (K141Q), HIS-PGAM5-K191R (K191R) or HIS-PGAM5-K191Q (K191Q) were subjected to an *in vitro* phosphatase assay. The enzyme activity data are expressed as the mean ± SD ($n = 3$) compared with the indicated group $^*P < 0.05$, ns, no significant difference. (F) Conserved analysis of the K191 site of PGAM5 from the indicated species.

inhibitor TSA, increased PGAM5 acetylation (Figure 2A), indicating that a member of the Sirtuin family of deacetylases is involved in PGAM5 deacetylation. As a transmembrane protein, PGAM5 is located in the outer membrane of mitochondria [17]. According to its secondary structure information, amino acids 1–6 are located inside the mitochondria, amino acids 7–29 belong to the transmembrane region and span the outer mitochondrial membrane, and amino acids 30–289 are located in the cytoplasm [11,18,19]. Because SIRT2 is mostly localized in the cytoplasm and K191 is the crucial acetylation site on PGAM5 (Figure 2B), we co-expressed PGAM5 with the cytosolic SIRT deacetylase SIRT2 [20]. We found that SIRT2 clearly bound to PGAM5 (Figure 2C). Furthermore,

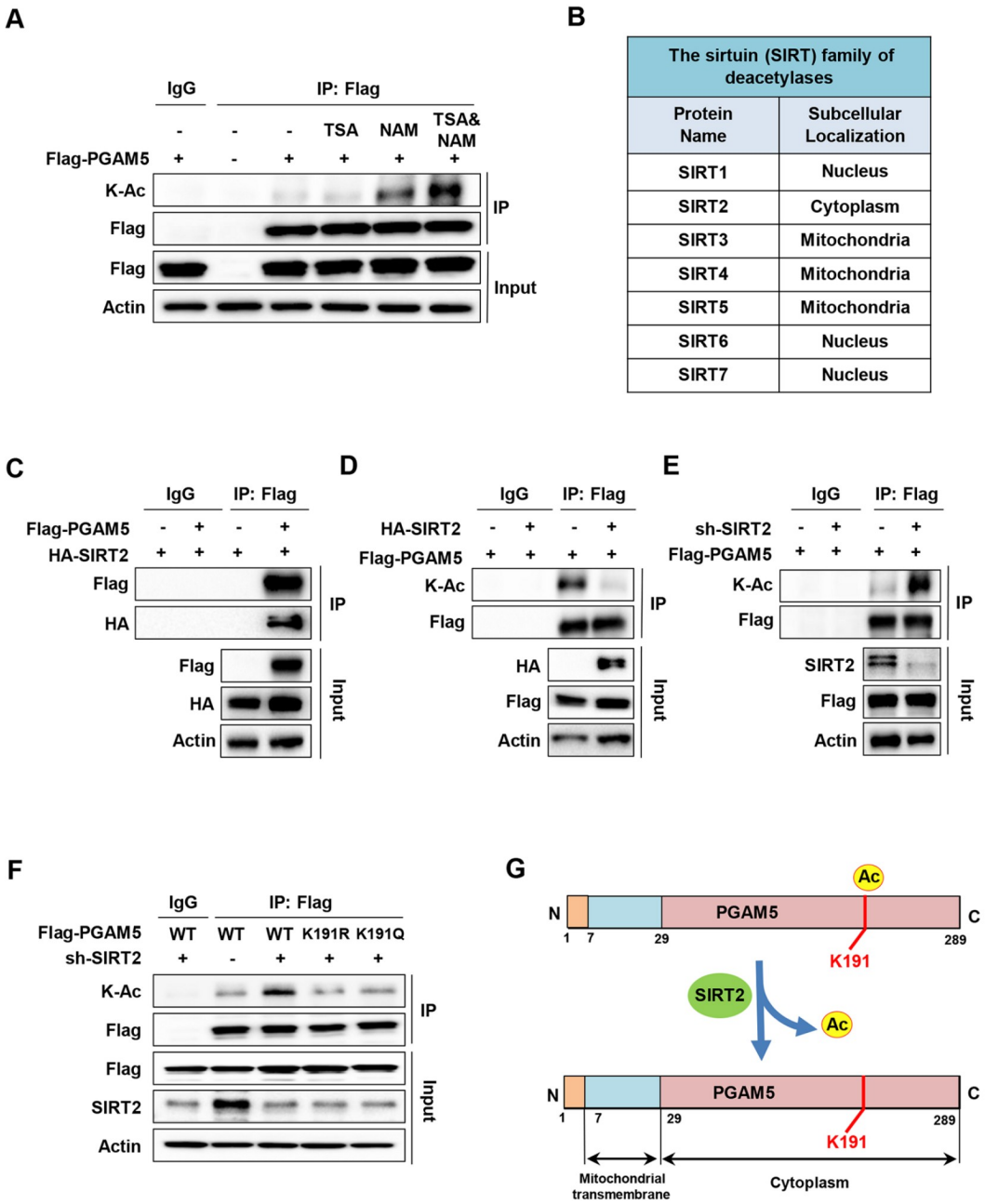

Figure 2. SIRT2 mediates PGAM5-K191 deacetylation (A) Flag-tagged PGAM5 was stably expressed in PLC cells treated with TSA and/or NAM, followed by immunoprecipitation using an anti-Flag antibody and western blot analysis of the lysine acetylation (K-Ac) of PGAM5. (B) Localization of sirtuin family deacetylases in cells. (C) Immunoprecipitation was performed using anti-Flag antibody or IgG in PLC cells. Flag-PGAM5 and HA-SIRT2 expression were determined by western blot analysis. (D) PLC cells stably expressing Flag-PGAM5 were further transfected with vectors expressing EV or HA-SIRT2. Immunoprecipitation was performed using an anti-Flag antibody or IgG in PLC cells. The acetylation of Flag-PGAM5 was detected by western blot analysis. (E) PLC cells stably expressing Flag-PGAM5 were further transfected with vectors expressing NTC or SIRT2 shRNA. Immunoprecipitation was performed using an anti-Flag antibody or IgG in PLC cells. The acetylation of Flag-PGAM5 was determined by western blot analysis. (F) PLC cells with stable knockdown of endogenous *PGAM5* were further transfected with vectors expressing Flag-PGAM5-WT, Flag-PGAM5-K191R and Flag-PGAM5-K191Q. The above cells were subsequently infected with viruses expressing NTC or SIRT2 shRNA. Immunoprecipitation was performed using an anti-Flag antibody or IgG in PLC cells. The acetylation of Flag-PGAM5 was detected by western blot analysis. (G) Diagram of the mechanism by which SIRT2 regulates the deacetylation of PGAM5-K191.

coexpression of SIRT2 reduced PGAM5 acetylation, while knockdown of *SIRT2* promoted PGAM5 acetylation (Figure 2D,E). To verify whether SIRT2 regulates PGAM5 acetylation at K191, we overexpressed wild-type PGAM5 as well as the K191R mutant and then knocked down *SIRT2* with shRNAs. Western blot analysis showed that *SIRT2* knockdown inhibited PGAM5 acetylation at K191 (Figure 2F). These results suggested that the deacetylation of PGAM5 at K191 is catalyzed by SIRT2 and demonstrated a specific and prominent role of SIRT2 in the K191 deacetylation of PGAM5 (Figure 2G).

SIRT2-mediated deacetylation of PGAM5^{K191} facilitates ME1 dephosphorylation and enhances ME1 activity

ME1 catalyzes the conversion of malate to pyruvate while simultaneously regenerating NADPH and plays a significant role in lipogenesis [21]. Recently, it was reported that PGAM5 mediates ME1 dephosphorylation, induces intracellular lipid metabolism and NADPH synthesis and promotes colorectal cancer cell proliferation [14]. However, whether the acetylation-mediated function of PGAM5 affects tumor metabolic reprogramming through ME1 remains unclear in liver cancer cells. Therefore, we confirmed the interaction between PGAM5 and ME1 by co-IP in HEK293T cells (Figure 3A). Subsequently, we also found that overexpression of PGAM5 dephosphorylated ME1 in PLC cells; in contrast, knockdown of *PGAM5* increased the phosphorylation level of ME1 (Supplementary Figure S1A,B). More interestingly, immunoprecipitation experiments showed that SIRT2 facilitates the binding of PGAM5 to ME1 in PLC cells (Figure 3B,C).

We next investigated whether acetylation of PGAM5 at K191 is involved in the regulation of ME1 phosphorylation level. In PLC cells co-overexpressing wild-type PGAM5, K191R or K191Q mutant together with ME1, we discovered that the K191Q mutant hindered PGAM5 binding to ME1 and accelerated ME1 phosphorylation (Figure 3D,E). In addition, the PGAM5 K191R mutant significantly decreased the phosphorylation level of ME1 but had no effect on the activation mutant of ME1 (ME1-S336A) (Figure 3E). More importantly, knockdown of *SIRT2* inhibited ME1 dephosphorylation and enzymatic activity in WT-PGAM5-expressing PLC cells but not in K191R- or K191Q-expressing cells or the ME1 phosphorylation level and enzymatic activity in ME1-S336A mutant cells (Figure 3F,G). Considering that the level of ME1 dimerization affects ME1 activity, our DSS crosslinking analysis revealed that over-expression of SIRT2 led to a decrease in ME1 monomer formation and a strong increase in ME1 dimer level (Supplementary Figure S2). Taken together, our data demonstrate that SIRT2-mediated PGAM5-K191 deacetylation facilitates ME1 dephosphorylation, leading to its upregulated enzyme activity.

Deacetylation of PGAM5 promotes lipid metabolism and tumor growth via dephosphorylating ME1

ME1 functions to promote one-carbon metabolism, pyruvate metabolism, NADPH and triglyceride (TG) synthesis in cells [22]. As we observed that PGAM5 deacetylation increased ME1 enzymatic activity, we next sought to explore whether acetylation of PGAM5 regulates the homeostasis of NADPH. We knocked down endogenous *PGAM5* and then re-expressed wild-type PGAM5 or the K191R or K191Q mutant in PLC cells (Figure 4A). As expected, we found that intracellular NADPH decreased under the knockdown of endogenous *PGAM5*. Furthermore, the restoration of wild-type PGAM5 and the K191R mutant, but not the K191Q mutant, significantly increased NADPH level (Figure 4B). In addition, the trend of TG level was similar to that of NADPH in the corresponding cells (Figure 4C). In addition, cell growth curves showed that the deacetylation mimic PGAM5-K191R, but not the K191Q mutant, significantly promoted PLC cell proliferation (Figure 4D).

To address whether the acetylation of PGAM5-K191 affects cellular NADPH and TG levels by regulating ME1-S336 phosphorylation. We knocked down endogenous *ME1* and re-expressed wild-type ME1 or ME1-S336A (activation mutant) in the above PLC cells (Figure 4E). ME1-S336A significantly increased the levels of NADPH and TG. However, the PGAM5-K191Q mutant reduced the levels of NADPH and TG in wild-type ME1 cells but not in ME1-S336A mutant cells (Figure 4F,G). Similarly, alterations in PGAM5 acetylation had no effect on the proliferation of PLC cells expressing the ME1 S336A mutant (Figure 4H). These data demonstrate that the deacetylation of PGAM5-K191 promotes NADPH production, lipid metabolism and tumor growth by dephosphorylating ME1. We also performed a xenograft assay to determine whether the deacetylation of PGAM5 promotes tumor growth *in vivo*. Compared to PGAM5-WT, PGAM5-191R increased tumor growth, while PGAM5-191Q significantly retarded cell growth *in vivo* (Figure 4I,J). Our data indicated that the post-translational acetylation of PGAM5 plays a crucial role in liver cancer cell development.

Discussion

Protein lysine acetylation is a common post-translational modification in cells [23–25]. More than 20% of the proteins localized in mitochondria undergo (de)acetylation modification [26]. Protein lysine-acetylation modification plays important biological roles in protein-protein interactions and protease activity, affecting protein subcellular localization and protein stability [6,27]. Aberrant protein lysine acetylation can alter a variety of cellular functions and play important roles under physiological and pathological conditions. PGAM5 is normally located on the mitochondrial outer membrane and has been implicated in a variety of cellular activities related to signal transduction pathways, such as regulating mitophagy, cellular oxidative stress, cell necrosis and apoptosis, fatty acid metabolism and NADPH synthesis [8,11,14,17,28,29]. However, the molecular mechanism of PGAM5 in the occurrence and development of liver cancer remains elusive. Our data demonstrated that the PGAM5 protein can be acetylated in cells, and its enzyme activity is inhibited by Lys 191 acetylation, which is mediated by the cytosolic deacetylase SIRT2 (Figures 1E and 2G).

Reprogramming metabolism is a major hallmark of cancer [30]. Altered lipid synthesis in particular plays an extremely critical role in tumor growth. Malic enzyme 1 (ME1) is an NADP(+)-dependent enzyme that generates NADPH for fatty acid biosynthesis by catalyzing the conversion of malate to pyruvate, thereby linking glycolysis and the TCA cycle. In this study, we demonstrated that the acetylation of PGAM5-K191 significantly inhibited PGAM5 binding to the substrate ME1, while the PGAM5-mimic deacetylation mutant (K191R) enhanced ME1 metabolic enzyme activity through ME1 dephosphorylation (Figure 3E,G). Furthermore, deacetylation of PGAM5 promoted NADPH production, triglyceride (TG) synthesis and tumor growth by dephosphorylating ME1 (Figure 4E,G).

SIRT2 is upregulated in many cancers, such as pancreatic cancer, breast cancer and hepatocellular carcinoma (HCC) [31–36], and the impact of SIRT2 on metabolism and possible molecular mechanisms in cancer cells still deserve further research. Our data showed that SIRT2 deacetylates the lysine K191 site of PGAM5 and induced the protein phosphatase activity of PGAM5, which dephosphorylated and activated ME1, ultimately leading to increased NADPH levels and lipid synthesis. Thus, activation of PGAM5 by SIRT2-mediated deacetylation showed tumor-promoting effects.

In conclusion, this study discovered and analyzed the molecular mechanism of PGAM5 deacetylation and the important role of the SIRT2-PGAM5-ME1 axis in the proliferation of liver cancer cells (Figure 5).

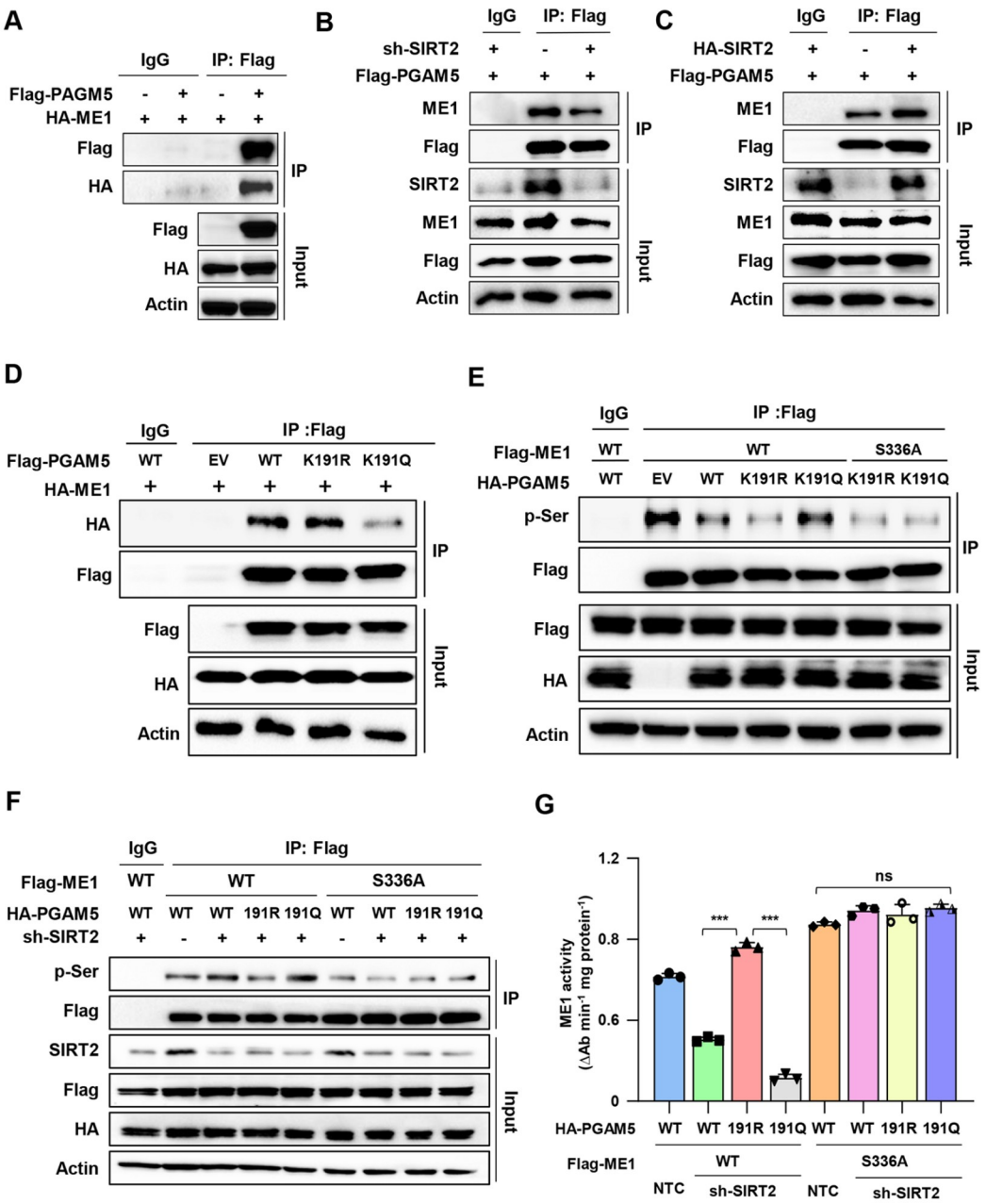

Figure 3. The deacetylation of PGAM5-K191 mediated by SIRT2 facilitates ME1 dephosphorylation and activity (A) Flag-PGAM5 and HA-ME1 were co-overexpressed in PLC cells. Immunoprecipitation was performed using an anti-Flag antibody or IgG, followed by western blot analysis of HA-ME1 and Flag-PGAM5. (B) PLC cells stably expressing Flag-PGAM5 were further transfected with vectors expressing NTC or SIRT2 shRNA. Immunoprecipitation was performed using an anti-Flag antibody or IgG in PLC cells. ME1 and Flag-PGAM5 were determined by western blot analysis. (C) PLC cells stably expressing Flag-PGAM5 were further transfected with empty vector (EV) or vectors expressing HA-SIRT2. Immunoprecipitation was performed using an anti-Flag antibody or IgG in PLC cells. ME1 and Flag-PGAM5 were determined by western blot analysis. (D) PLC cells with stable knockdown of endogenous *PGAM5* were further transfected with EV or vectors expressing Flag-wild-type-PGAM5, Flag-PGAM5-K191R and Flag-PGAM5-K191Q. The above cells were subsequently infected with viruses expressing HA-ME1. Immunoprecipitation was performed using an anti-Flag antibody or IgG in PLC cells. Flag-PGAM5 and HA-ME1 were determined by western blot analysis. (E) PLC cells with stable knockdown of endogenous *PGAM5* were further transfected with EV or vectors expressing HA-PGAM5, HA-PGAM5-K191R and HA-PGAM5-K191Q. The above cells were knocked down with ME1 shRNA and were subsequently infected with viruses expressing Flag-ME1-WT or Flag-ME1-S336A. Immunoprecipitation was performed using an anti-Flag antibody or IgG in PLC cells. Phosphorylation of ME1, Flag-ME1 and HA-PGAM5 was determined by western blot analysis. (F) PLC cells with stable knockdown of endogenous *PGAM5* were further transfected with vectors expressing PGAM5-WT, PGAM5-K191R and PGAM5-K191Q. The above cells were knocked down with ME1 shRNA and were subsequently infected with viruses expressing Flag-ME1-WT or Flag-ME1-S336A. Meanwhile, the cells were infected with the viruses expressing NTC or SIRT2 shRNA. Immunoprecipitation was performed using an anti-Flag antibody or IgG in the above cells. Phosphorylation of ME1, Flag-ME1, HA-PGAM5 and SIRT2 was detected by western blot analysis. (G) The metabolic enzyme activity of ME1 was detected by a kit assay in the PLC cells used in (F). The enzyme activity data are expressed as the mean ± SD ($n = 3$) and compared with the corresponding groups. $^*P < 0.05$, ns, no significant difference.

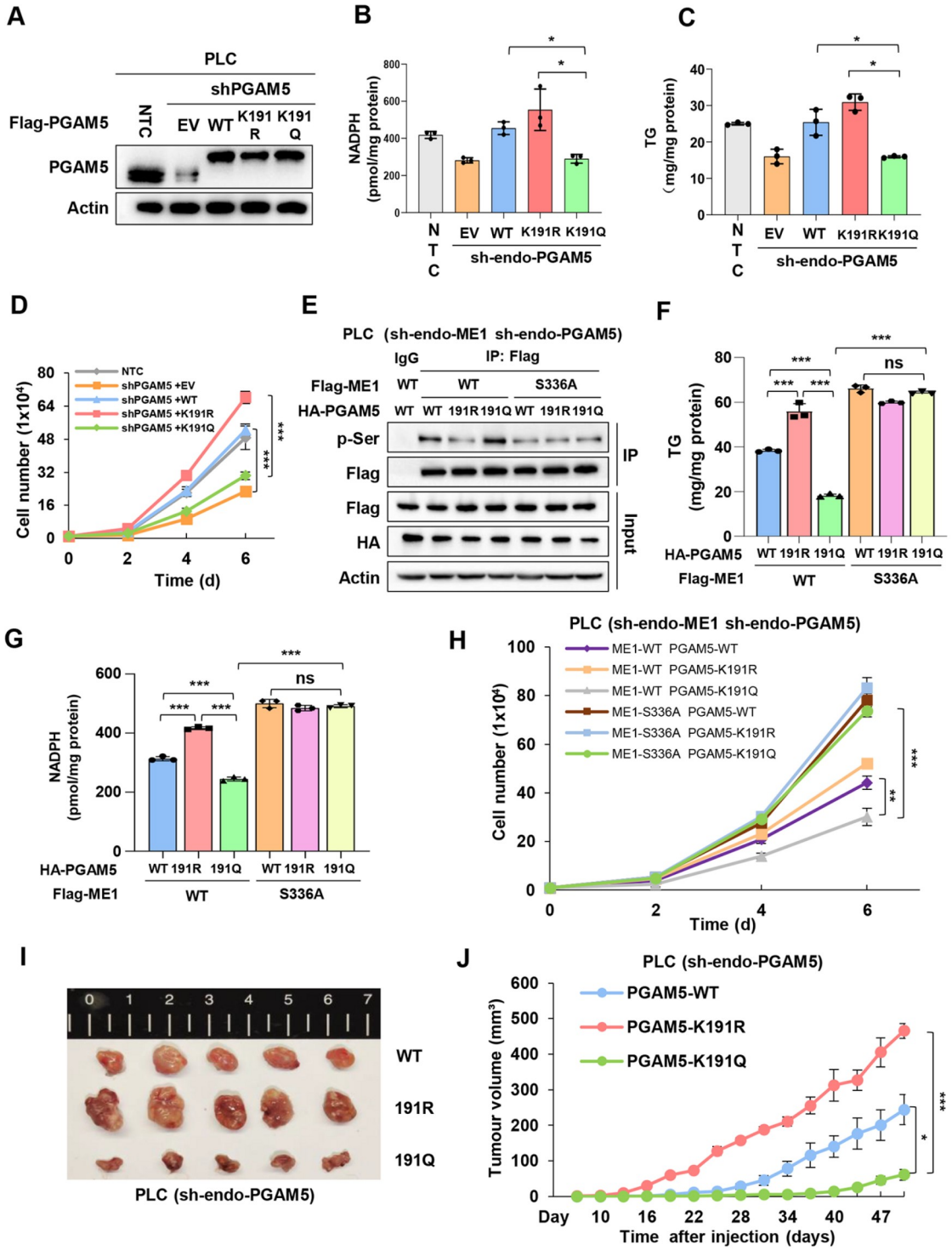

Figure 4. Deacetylation of PGAM5 promotes lipid metabolism and tumor growth by dephosphorylating ME1 (A–D) PLC cells with stable knockdown of endogenous *PGAM5* were further transfected with EV or vectors expressing Flag-PGAM5-WT, Flag-PGAM5-K191R and Flag-PGAM5-K191Q, followed by western blot analysis of PGAM5 (A). The intracellular NADPH (B) and TG (C) contents were determined in the above cells (A). The growth of PLC cells was determined by trypan blue staining (D). (E–H) The PLC cells used in (A) were further knocked down for endogenous *ME1* and then re-expressed ME1-WT or ME1-S336A. The indicated protein levels were determined by western blot analysis (E). The intracellular NADPH (F) and TG (G) levels were determined in the above cells (E). The growth of PLC cells was determined by trypan blue staining (H). Data are presented as the mean ± SD ($n = 3$, each group) and compared with the corresponding groups. *$P < 0.05$, ns, no significant difference. (I,J) PLC cells stably expressing PGAM5-WT, PGAM5-K191R or PGAM5-K191Q with endogenous PGAM5 knockdown were injected subcutaneously into nude mice ($n = 5$ for each group). Tumor growth curves were measured starting 7 days after injection (I), and tumors were extracted and compared at the end of the experiment (J). Data are presented as the mean ± SD ($n = 5$, each group) and compared with the corresponding groups. *$P < 0.05$. ns, no significant difference.

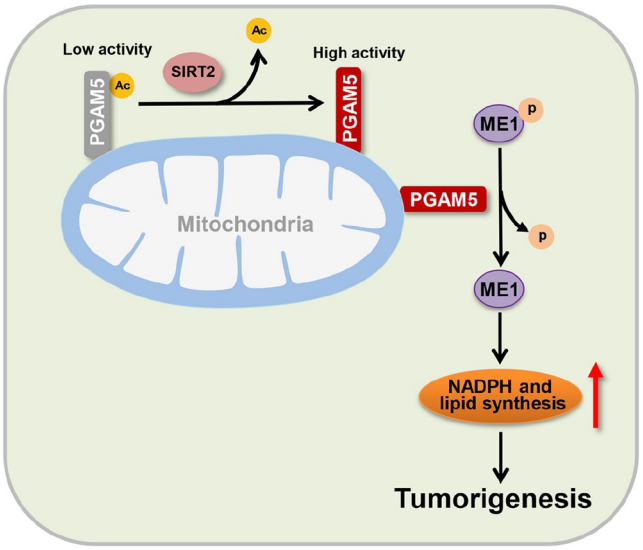

Figure 5. PGAM5 deacetylation mediated by SIRT2 facilitates lipid metabolism and liver cancer proliferation Schematic showing that deacetylation-dependent activation of PGAM5 by SIRT2. Consequently, activation of PGAM5 leads to ME1 dephosphorylation, which triggers TG and NADPH accumulation and liver cancer proliferation.

Supplementary Data

Supplementary data is available at *Acta Biochimica et Biophysica Sinica* online.

Funding

This work was supported by the grants from the National Natural Science Foundation of China (Nos. 81930083, 82192893, 82103363, and 81821001), the Chinese Academy of Sciences (No. XDB39000000), the National Key R&D Program of China (No. 2022YFA1304504), the Institute of Health and Medicine, Hefei Comprehensive National Science Center (No. DJK-LX-2022001), the Fundamental Research Funds for the Central Universities (No. YD2070002008), and the China Postdoctoral Science Foundation (No. 2021M700898).

Conflict of Interest

The authors declare that they have no conflict of interest.

References

1. Kim SC, Sprung R, Chen Y, Xu Y, Ball H, Pei J, Cheng T, *et al.* Substrate and functional diversity of lysine acetylation revealed by a proteomics survey. *Mol Cell* 2006, 23: 607–618
2. Choudhary C, Kumar C, Gnad F, Nielsen ML, Rehman M, Walther TC, Olsen JV, *et al.* Lysine acetylation targets protein complexes and co-regulates major cellular functions. *Science* 2009, 325: 834–840
3. Zhao S, Xu W, Jiang W, Yu W, Lin Y, Zhang T, Yao J, *et al.* Regulation of cellular metabolism by protein lysine acetylation. *Science* 2010, 327: 1000–1004
4. Wang Q, Zhang Y, Yang C, Xiong H, Lin Y, Yao J, Li H, *et al.* Acetylation of metabolic enzymes coordinates carbon source utilization and metabolic flux. *Science* 2010, 327: 1004–1007
5. Xiong Y, Guan KL. Mechanistic insights into the regulation of metabolic enzymes by acetylation. *J Cell Biol* 2012, 198: 155–164
6. Ellmeier W, Seiser C. Histone deacetylase function in CD4+ T cells. *Nat Rev Immunol* 2018, 18: 617–634
7. Takeda K, Komuro Y, Hayakawa T, Oguchi H, Ishida Y, Murakami S, Noguchi T, *et al.* Mitochondrial phosphoglycerate mutase 5 uses alternate catalytic activity as a protein serine/threonine phosphatase to activate ASK1. *Proc Natl Acad Sci USA* 2009, 106: 12301–12305
8. He GW, Günther C, Kremer AE, Thonn V, Amann K, Poremba C, Neurath MF, *et al.* PGAM5-mediated programmed necrosis of hepatocytes drives acute liver injury. *Gut* 2017, 66: 716–723
9. Panda S, Srivastava S, Li Z, Vaeth M, Fuhs SR, Hunter T, Skolnik EY. Identification of PGAM5 as a mammalian protein histidine phosphatase that plays a central role to negatively regulate CD4+ T cells. *Mol Cell* 2016, 63: 457–469
10. Ramachandran A, Jaeschke H. PGAM5: a new player in immune-mediated liver injury. *Gut* 2017, 66: 567–568
11. Wang Z, Jiang H, Chen S, Du F, Wang X. The mitochondrial phosphatase PGAM5 functions at the convergence point of multiple necrotic death pathways. *Cell* 2012, 148: 228–243
12. Cheng J, Qian D, Ding X, Song T, Cai M, Dan Xie M, Wang Y, *et al.* High PGAM5 expression induces chemoresistance by enhancing Bcl-xL-mediated anti-apoptotic signaling and predicts poor prognosis in hepatocellular carcinoma patients. *Cell Death Dis* 2018, 9: 991–1007
13. Ng Kee Kwong F, Nicholson AG, Pavlidis S, Adcock IM, Chung KF. PGAM5 expression and macrophage signatures in non-small cell lung cancer associated with chronic obstructive pulmonary disease (COPD). *BMC Cancer* 2018, 18: 1238–1247
14. Zhu Y, Gu L, Lin X, Liu C, Lu B, Cui K, Zhou F, *et al.* Dynamic regulation of ME1 phosphorylation and acetylation affects lipid metabolism and colorectal tumorigenesis. *Mol Cell* 2020, 77: 138–149.e5
15. Li ST, Huang D, Shen S, Cai Y, Xing S, Wu G, Jiang Z, *et al.* Myc-mediated SDHA acetylation triggers epigenetic regulation of gene expression and tumorigenesis. *Nat Metab* 2020, 2: 256–269
16. Liang S, Zhu C, Suo C, Wei H, Yu Y, Gu X, Chen L, *et al.* Mitochondrion-localized SND1 promotes mitophagy and liver cancer progression through PGAM5. *Front Oncol* 2022, 12: 857968
17. Cheng M, Lin N, Dong D, Ma J, Su J, Sun L. PGAM5: A crucial role in mitochondrial dynamics and programmed cell death. *Eur J Cell Biol* 2021, 100: 151144
18. Lo SC, Hannink M. PGAM5 tethers a ternary complex containing Keap1 and Nrf2 to mitochondria. *Exp Cell Res* 2008, 314: 1789–1803
19. Wilkins JM, McConnell C, Tipton PA, Hannink M. A conserved motif mediates both multimer formation and allosteric activation of phosphoglycerate mutase 5. *J Biol Chem* 2014, 289: 25137–25148
20. Mei Z, Zhang X, Yi J, Huang J, He J, Tao Y. Sirtuins in metabolism, DNA repair and cancer. *J Exp Clin Cancer Res* 2016, 35: 182–196
21. Jiang P, Du W, Mancuso A, Wellen KE, Yang X. Reciprocal regulation of p53 and malic enzymes modulates metabolism and senescence. *Nature* 2013, 493: 689–693
22. Lu YX, Ju HQ, Liu ZX, Chen DL, Wang Y, Zhao Q, Wu QN, *et al.* ME1 regulates NADPH homeostasis to promote gastric cancer growth and metastasis. *Cancer Res* 2018, 78: 1972–1985
23. Diallo I, Seve M, Cunin V, Minassian F, Poisson JF, Michelland S, Bourgoin-Voillard S. Current trends in protein acetylation analysis. *Expert Rev Proteomics* 2019, 16: 139–159
24. Gil J, Ramírez-Torres A, Encarnación-Guevara S. Lysine acetylation and cancer: A proteomics perspective. *J Proteomics* 2017, 150: 297–309
25. Morales-Tarré O, Alonso-Bastida R, Arcos-Encarnación B, Pérez-Martínez L, Encarnación-Guevara S. Protein lysine acetylation and its role in different human pathologies: a proteomic approach. *Expert Rev Proteomics* 2021, 18: 949–975
26. Baeza J, Smallegan MJ, Denu JM. Mechanisms and dynamics of protein

acetylation in mitochondria. *Trends Biochem Sci* 2016, 41: 231–244
27. Marín-Hernández Á, Rodríguez-Zavala JS, Jasso-Chávez R, Saavedra E, Moreno-Sánchez R. Protein acetylation effects on enzyme activity and metabolic pathway fluxes. *J Cell Biochem* 2022, 123: 701–718
28. Bernkopf DB, Jalal K, Brückner M, Knaup KX, Gentzel M, Schambony A, Behrens J. PGAM5 released from damaged mitochondria induces mitochondrial biogenesis via Wnt signaling. *J Cell Biol* 2018, 217: 1383–1394
29. Rauschenberger V, Bernkopf DB, Krenn S, Jalal K, Heller J, Behrens J, Gentzel M, *et al.* The phosphatase PGAM5 antagonizes Wnt/β-Catenin signaling in embryonic anterior-posterior axis patterning. *Development* 2017, 144: 2234–2247
30. Hanahan D, Weinberg RA. Hallmarks of cancer: the next generation. *Cell* 2011, 144: 646–674
31. Zhao D, Mo Y, Li MT, Zou SW, Cheng ZL, Sun YP, Xiong Y, *et al.* NOTCH-induced aldehyde dehydrogenase 1A1 deacetylation promotes breast cancer stem cells. *J Clin Invest* 2014, 124: 5453–5465
32. Zhao D, Zou SW, Liu Y, Zhou X, Mo Y, Wang P, Xu YH, *et al.* Lysine-5 acetylation negatively regulates lactate dehydrogenase A and is decreased in pancreatic cancer. *Cancer Cell* 2013, 23: 464–476
33. Lin R, Tao R, Gao X, Li T, Zhou X, Guan KL, Xiong Y, *et al.* Acetylation stabilizes ATP-citrate lyase to promote lipid biosynthesis and tumor growth. *Mol Cell* 2013, 51: 506–518
34. Huang S, Zhao Z, Tang D, Zhou Q, Li Y, Zhou L, Yin Y, *et al.* Downregulation of SIRT2 inhibits invasion of hepatocellular carcinoma by inhibiting energy metabolism. *Transl Oncol* 2017, 10: 917–927
35. Zhang M, Pan Y, Dorfman RG, Yin Y, Zhou Q, Huang S, Liu J, *et al.* Sirtinol promotes PEPCK1 degradation and inhibits gluconeogenesis by inhibiting deacetylase SIRT2. *Sci Rep* 2017, 7: 7
36. Chen J, Chan AWH, To KF, Chen W, Zhang Z, Ren J, Song C, *et al.* SIRT2 overexpression in hepatocellular carcinoma mediates epithelial to mesenchymal transition by protein kinase B/glycogen synthase kinase-3β/β-catenin signaling. *Hepatology* 2013, 57: 2287–2298